An Investigation into the Structural, Electronic, and Non-Linear Optical Properties in C N (N=20, 24, 26, 28, 30, 32, 34, 36, and 38) Fullerene Cages

K. Soyarslan
Gazi University
B. Ortatepe
Gazi University
B. Yurduguzel
Kaman Technical Vocational School of Higher Education, Ahi Evran University
M. T. Güllüoğlu
Harran University
Y. Erdogdu (yerdogdu@gazi.edu.tr)
Gazi University

Research Article

Keywords: DFT, Fullerenes, Non-linear optical properties, HOMO, LUMO energies.

Posted Date: August 1st, 2022

DOI: https://doi.org/10.21203/rs.3.rs-1893282/v1

Abstract

The present study attempts to investigate the structural, electronic, and non-linear optical properties of C_N (N = 20, 24, 26, 28, 30, 32, 34, 36, and 38) fullerene cages based on Density Functional Theory (DFT). In the DFT calculations, the B3LYP/6-311G(d,p) and CAM-B3LYP/6-311 + + G(d,p) level of theories were used. The isomers of each fullerene have been received from the Fullerene Structure Library. These isomers have optimized using the B3LYP/6-311G(d,p). The results included optimization of the neutral, and ionic state structures according to their multiplicity. Geometries, optimization energies, relative energies, frequencies, HOMO, LUMO, and HOMO-LUMO gap of these stable fullerene cages have been predicted by B3LYP/6-311G(d,p). Afterwards, the most stable structures have been re-optimized using the CAM-B3LYP /6-311 + + G(d,p). Finally, non-linear optical properties, fukui functions, density of state, electron affinity, ionization potential values of the most stable fullerene cages have been found out by the DFT/ CAM-B3LYP /6-311 + + G(d,p) level of theory. All calculation results have been compared with both C60 fullerene and the relevant literature on corresponding fullerenes.

1. Introduction

Organic nanostructures such as fullerenes, nanotubes, and graphene generally receive much attention among the scholars. The main reason behind this is that organic nanostructures has properties suitable for practically various applications in different scientific fields. Among these organic nanostructures, fullerenes have outstanding properties in many different fields. With the discovery of the C_{60} fullerene by Kroto [1], an array of theoretical and experimental studies has been carried out to determine the physical and chemical properties of fullerenes, thereby characterizing a wide range of fullerenes over the years [2–4].

Currently, fullerenes find wide development application for modern science such as physics, medicine, materials science, and biology. More specifically, they have wide applications in many fields such as organic solar cells, super-capacitors, catalyzers, and superconducting materials. In addition to these properties, nano-size and thermally stable fullerenes have a wide range of applications in electronics, photonics, and nonlinear optics due to their electronic, sensing, and optical properties. The fact that fullerenes have all these application areas is due to their properties. For instance, they have a high electron affinity, unique geometric structure, electronic, and physicochemical properties. Among these properties, high electron affinity is one of its most important properties. Thanks to this property, it can have the ability to attract extra electrons and form a bound mono or poly-anion. Besides, it is nanostructures that have applications in artificial photosynthesis and photovoltaic devices [5].

Despite all the theoretical and experimental studies, there are still many deficiencies in the characterization of fullerenes. So, theoretical and experimental characterization studies of fullerenes are still critical. The aim of this study is to determine the structural, electronic, and nonlinear optical properties of C_N (N = 20, 24, 26, 28, 30, 32, 34, 36, and 38) fullerene cages. This study provided the theoretical calculation results of C_N fullerene cages have been presented. To the best of our knowledge, a

comparative study of these fullerenes is not reported in the literature yet. To fill such a void, structural, electronic, and non-linear optical properties analyses of these fullerenes are provided in the manuscript in detail. All isomers of C_N fullerenes with various spin multiplicities were simulated by Density Functional Theory (DFT). Finally, a detailed study of the Mulliken charge, density of state, and Fukui function of these fullerenes has been presented.

2. Method Of Calculation

The researchers performed DFT calculations with Gaussian 16 code [6]. The B3LYP [7,8], CAM-B3LYP [9] functionals were employed in the DFT calculations. They used combinations of the 6-311G(d,p)[10] and 6-311 + + G(d,p) basis sets with the functionals above in the calculations.

Firstly, the geometric optimization of all isomers of each fullerene cages were carried out by using the B3LYP/6-311G(d,p) (abbreviated as DFT/B3LYP level). The geometries of all fullerene cages were taken from the Fullerene Structure Library built by Mitsuho Yoshida [11]. Harmonic vibration frequencies at the same level were also calculated to check the stability of the geometries on the potential energy surface. Electrostatic potential maps, HOMO, and LUMO plots from results of the optimization calculations of the most stable structure of each fullerene cage were visualized with the same level.

Later, the CAM-B3LYP/6-311 + + G(d,p) (abbreviated as DFT/CAM-B3LYP level) were used on non-linear optical properties, Mulliken atomic charge, density of state and Fukui function calculations. Since ionization potentials (IP) and electron affinities (EA) are essential properties that reflect the stability of fullerene cages, IP and EA were calculated from the optimization energies of the most stable geometries of neutral and charged fullerene cages [12]. The IP was obtained by considering the difference between the optimized energies of the neutral fullerene cages and their cations. In this study, we evaluated the IP versus fullerene cage size.

IP = E(optimized cation)-E(optimized neutral) (1)

EA is defined as the energy obtained when an electron is added to the isolated atom. Adiabatic electron affinity (EA_{ad}) values for the lowest energy isomers of fullerene cages were computed in this study. The EA_{ad} is defined as the optimization energy difference in the most stable neutral and anion state [12].

EA_{ad}=E(optimized neutral)-E(optimized anion) (2)

The vertical electron affinity (EA_{vert}) is the energy difference between the optimized neutral state and the anionic state without changing the geometry in the neutral state [12].

EA_{vert}=E(optimized neutral)-E(anion at optimized neutral geometry) (3)

The vertical detachment energy (VDE) is the energy required to remove an electron from the anionic fullerene cages without changing its geometry. As understood from the definition, it is regarded as the

energy difference between the neutral state without changing the geometry in the optimized anionic state and the optimized anion state [12].

VDE = E(neutral at optimized anion geometry)-E(optimized anion) (4)

It is important to determine the nonlinear optical properties of fullerenes. Theoretically, making (hyper)polarizability calculations might provide data for future studies of fullerenes. The energy of a system in the weak and homogeneous electric field can be defined as:

$$E = E^0 - \mu_\alpha F_\alpha - \frac{1}{2}\alpha_{\alpha\beta}F_\alpha F_\beta - \frac{1}{6}\beta_{\alpha\beta\gamma}F_\alpha F_\beta F_\gamma - \dots$$

5

where E^0 is the total molecular energy in the absence of an electric field. F_α is the electric field component along the α direction. The μ_α, $\alpha_{\alpha\beta}$, and $\beta_{\alpha\beta\gamma}$ denote dipole moment, polarizability and the first order hyperpolarizability respectively [13]. The dipole moment (μ), the mean polarizability ($\bar{\alpha}$), the anisotropy of the polarizability ($\Delta\alpha$), and the first order hyperpolarizability (β_0) are defined as;

$$\mu^2 = \mu_x^2 + \mu_y^2 + \mu_z^2$$

6

$$\bar{\alpha} = \left(\alpha_{xx} + \alpha_{yy} + \alpha_{zz}\right)/3$$

7

$$\Delta\alpha = \frac{1}{\sqrt{2}}\left[\left(\alpha_{xx} - \alpha_{yy}\right)^2 + \left(\alpha_{yy} - \alpha_{zz}\right)^2 + \left(\alpha_{zz} - \alpha_{xx}\right)^2 + 6\left(\alpha_{xy}^2 + \alpha_{yz}^2 + \alpha_{xz}^2\right)\right]^{1/2} \quad (8)$$

$$\beta_x = \beta_{xxx} + \beta_{xyy} + \beta_{xzz}$$

9

$$\beta_y = \beta_{yyy} + \beta_{yzz} + \beta_{yxx}$$

10

$$\beta_z = \beta_{zzz} + \beta_{zxx} + \beta_{zyy}$$

11

$$\beta_0 = \left[\left(\beta_{xxx} + \beta_{xyy} + \beta_{xzz}\right)^2 + \left(\beta_{yyy} + \beta_{xxy} + \beta_{yzz}\right)^2 + \left(\beta_{zzz} + \beta_{xxz} + \beta_{yyz}\right)^2\right]^{1/2} \quad (12)$$

In general, the main purpose of Molecular Electrostatic Potential (MEP) maps is to explain the charge distribution of the working system. In this calculation, a map was created due to the properties of the nucleus and the nature of the electrostatic potential energy. These visualizations were used to illustrate concepts such as polarity, electronegativity, and similar properties. These maps were sampled over the entire accessible surface of the studied structure. The three-dimensional isosurfaces of MEPs showed electrostatic potentials superimposed on a surface of electron density. The most negative electrostatic potential was shown in red while the most positive electrostatic potential was presented in blue [14].

Fukui function is an important concept in conceptual DFT, and it has been widely used in prediction of reactive site. It is also used as a descriptor in quantitative structure–activity relationships. It calculated with the help of the following equations. In these equations, q_k is the atomic charge at the r_{th} atomic site. The N, N + 1, and N-1 impressions show neutral, anionic, and cationic states, respectively. [14].

$$f_k^+ = q_k(N+1) - q_k(N) \quad \text{for nucleophilic attack (13)}$$

$$f_k^- = q_k(N) - q_k(N-1) \quad \text{for electrophilic attack (14)}$$

$$f_k^0 = \frac{1}{2}\left[q_k(N+1) - q_k(N-1)\right] \quad \text{for neutral (radical) attack (15)}$$

Euler's theorem [15] provides a rule for pentagonal and hexagonal numbers for C_{20} cage fullerene and fullerenes with an even number of atoms greater than C_{20} cage. C_{nm} (n≥2; m: even numbers) fullerene cages have twelve pentagons. The number of hexagons was determined by the expression (n/2–10). Pentagonal and hexagonal numbers were given in the correspond table for each fullerene.

3. Results And Discussions

The present study investigates the structural, electronic, and non-linear optical properties of neutral, cationic (single positive charge), and anionic (single negative charge) fullerenes. Geometry optimization of the neutral and charged states with different spin multiplicities was carried out for each of the fullerenes. The lowest-energy structures of these fullerenes were shown in Figs. 1–9. Pentagon/Hexagon numbers, symmetry, the optimized energies, and relative energies of all isomer of the fullerene cages with various spin multiplicities were given in Tables S1-S9. The results were discussed in the following sections.

- Position of Table 1
- Position of Table 2

Table 1
Ionization Potentials, Electron Affinities, Vertical Electron Affinity and vertical detachment energy of C_N and C_M fullerene cage by CAM-B3LYP/6-311 + + G(d,p)

	C_{20}	C_{24}	C_{26}	C_{28}	C_{30}	C_{32}	C_{34}	C_{36}	C_{38}
IP*	7.142	7.691	7.443	8.349	7.808	8.178	7.450	7.335	7.278
EA_{ad}*	2.391	3.252	2.618	2.864	3.559	3.025	2.955	2.889	2.957
EA_{vert}*	2.089	3.091	2.452	2.733	3.385	2.769	3.062	2.815	2.775
VDE*	2.699	3.572	2.815	3.007	3.689	3.305	3.163	2.962	3.143
*All values are in eV units.									

Table 2
Dipole moment (Debye), the mean polarizability ($\bar{\alpha}$), the anisotropy of the polarizability ($\Delta\alpha$) and the mean first order hyperpolarizability (β_0) of neutral C_N and C_M fullerene cages by CAM-B3LYP/6-311 + + G(d,p)

	C_{20}	C_{24}	C_{26}	C_{28}	C_{30}	C_{32}	C_{34}	C_{36}	C_{38}
μ*	0.000	0.000	0.000	0.000	0.119	0.000	0.113	0.000	0.033
$\bar{\alpha}$**	27.59	32.04	34.14	35.99	40.15	43.43	46.06	47.56	49.95
Δα **	1.552	8.242	5.588	0.000	5.438	8.035	8.103	0.909	5.917
β_x ***	0.000	0.000	0.000	0.000	-0.600	0.000	0.000	0.000	0.000
β_y ***	0.000	0.000	0.000	0.000	-1.289	0.000	0.000	0.000	0.000
β_z ***	0.000	0.000	0.000	0.000	-1.493	0.000	-2.656	0.000	-0.289
β_0 ***	0.000	0.000	0.000	0.000	2.062	0.000	2.656	0.000	0.289
*The dipole moment is in Debye units.									
**The mean polarizability, the anisotropy of the polarizability is in (10^{-24}) esu units. (1 a.u. = 0.1482 x10^{-24} esu)									
***The mean first order hyperpolarizability is in (10^{-30}) esu units. (1 a.u.= 8.6393x10^{-33} esu)									

3.1. C_{2N} (N:0, 4, 6, and 8) fullerenes

Fullerenes are closed-cage carbon structures consisting of 12 pentagons and certain number of hexagons. For each fullerene, the possible hexagon numbers could be 0, 2, 3, 4, 5, and more. The structure consisting of 12 pentagons without hexagons is the smallest possible fullerene. Thus, the smallest theoretically possible fullerene is C_{20}. The C_{20} with a dodecahedral cage structure is regarded as the smallest fullerene existing. It only comprises 12 pentagons and 30 bonds. Kroto [1] expressed the pentagon isolation rule, which stipulates that the most stable fullerenes should have 12 pentagons and that these pentagons should be as far apart as possible. Considering this rule, the C_{20} fullerene cage should be highly unstable. It is sometimes called “unconventional fullerene”.

The structure of the C_{20} fullerene cage has I_h symmetry. Besides, the C_{20} fullerene cage also has eight structures with subgroup symmetry. Wang [16] et al. reported that a symmetry path from I_h symmetry to C_1 symmetry found for C_{20} fullerene cage. Based on this result, the structure with D_{2h} symmetry is the most stable in this path. We took Wang's suggestion for the C_{20} as a starting point. However, negative frequency was detected in the structure's calculation with D_{2h} symmetry. Therefore, the calculations were continued with the structure with D_2 symmetry. It is structurally very similar between the structure with D_2 symmetry and the structure with D_{2h} symmetry. We have done all the following calculations for the C_{20} fullerene cage with geometry D_2. Table S1 presented all calculation results such as optimization energy for each multiplicity, symmetry, and geometry. The results showed that the most stable state of C_{20} fullerene obtained the singlet spin multiplicity for neutral state and quartet spin multiplicity for ionic cases. Figure 1 demonstrated the optimized geometry (a), Mulliken charge distribution (b), MEP counter (c), and HOMO-LUMO plot (d) of the most stable isomer of the C_{20} fullerene cage.

As seen in Fig. 1, the distribution of Mulliken charges was formed as 0.433 a.u. (eight atoms in green color), -0.409 a.u. (four red atoms on the top and bottom), -0.312 a.u. (four red atoms on the side edges), and − 0.143 a.u. (four atoms in dark red color). Figure 1 shows the gaps between the highest occupied molecular orbital (HOMO) and the lowest unoccupied molecular orbital (LUMO) plots. The researchers calculated at -5.442 eV (HOMO energy), -3.506 eV (LUMO energy), and 1.937 eV (HOMO-LUMO gap energy) by DFT/B3LYP level.

Prinzbach [17] et al. accomplished the first synthesis of C_{20}. In their study, $C_{20}H_{20}$ was firstly converted to $C_{20}Br_{20}$ by substitution of H atoms with Br atoms. Then, $C_{20}Br_{20}$ was debrominated to synthesize C_{20} fullerene. Apart from this study, many studies have been carried out on the synthesis of C_{20} [18]. Prinzbach [17] et al. reported that the C_{20} fullerene had an EA of 2.25 eV by its photoelectron spectrum. In other studies on EA of the C_{20} fullerene cage, this value was determined as 2.7 eV by Yang [19] et al. 2.65 eV by Wang [20] et al., and 2.689 eV by Wang [21] et al. According to the results from our calculations, 2.391 eV was predicted as EA of C_{20} fullerene cage by DFT/CAM-B3LYP level (Table 1). The C_{20} fullerene cage has a very symmetrical structure. As seen in Table 1, the μ and β_0 components of the C_{20} fullerene cage are all zero. However, the C_{20} fullerene has relatively small polarizability. The $\bar{\alpha}$ and the $\Delta\alpha$ were predicted at 27.59×10^{-24} esu and 1.552×10^{-24} esu by DFT/CAM-B3LYP level, respectively.

- Position of Fig. 1

Table 2S provides all calculation results such as optimization energy for each multiplicity, symmetry, and geometry for C_{24} fullerene cage. Considering the optimized geometry in Table S2, C_{24} fullerene cage comprises two hexagons at the top and bottom, and 12 pentagons at the waist. The fullerene possesses ideal D_{6d} symmetry [22]. As a starting point of the study, the C_{24} fullerene cage with D_{6d} symmetry was optimized. However, negative frequency was obtained in the structure's calculation with D_{6D} symmetry. Jensen [22] et al. noted that this structure with D_{6d} symmetry is stable geometry. Nevertheless, it was found that C_{24} fullerene cage with D_{6d} was in the transition structure in the calculations made on $D_{H(D)}$ and 6-31G (d) basis sets. Similarly, it was determined that C_{24} fullerene cage with D_{6d} was in a transition structure in our studies. Hence, the C_{24} symmetry was reduced from D_{6d} to D_6 symmetry. The C_{24} fullerene cage with D_{6d} and its D_6 symmetric structure were very similar structurally. In that symmetry, C_{24} fullerene cage with D_6 was the most stable. We noted that the most stable state of C_{24} fullerene cage determined the singlet spin multiplicity for neutral state, doublet spin multiplicity for anionic case, and quartet spin multiplicity for cationic case. Figure 2 showed the optimized geometry (a), Mulliken charge distribution (b), MEP counter (c), and HOMO-LUMO plot (d) of the most stable isomer of the C_{24} fullerene cage.

As seen in Fig. 2, the Mulliken charge of the atoms shown in red color is -0.148 a.u., and the charge of atoms shown in green color is 0.148 a.u. by DFT/CAM-B3LYP level. If the Mulliken charge distribution is examined, it could be seen that two different charges are distributed symmetrically. The researchers calculated at -6.050 eV (HOMO energy), -4.221 eV (LUMO energy) and 1.829 eV (HOMO-LUMO gap energy) by DFT/B3LYP level.

Janjanpour [23] et al. reported that the EA and IP of the C_{24} fullerene cage were predicted at 7.47 eV and 2.98 eV by B3LYP/6–31 + G (d). In the present study, the computed IP, $EA_{ad,}$ and VDE values were obtained at 7.691 eV, 3.252 eV and 2.699 eV by means of DFT/CAM-B3LYP, respectively (Table 1). The results showed that C_{24} fullerene cage obtained a great EA_{vert} value at 3.091 eV by DFT/CAM-B3LYP level. It indicated that C_{24} fullerene cage was a great electron acceptor.

The most stable geometry of the C_{24} fullerene cage possesses D_6 symmetry group. Given this structure, it could be stated that C_{24} had a very symmetrical structure. So, μ and β_0 components of the C_{24} fullerene cage were all zero. Kosar [24] et al. reported that $\bar{\alpha}$ of the C_{24} fullerene cage theoretically obtained 31.863 $x10^{-24}$ esu (215 a.u.) by B3LYP/6–31 + G(d) level. In the present study, $\bar{\alpha}$ and $\Delta\alpha$ were predicted at $32.04x10^{-24}$ esu, $8.242x10^{-24}$ esu by DFT/CAM-B3LYP level (Table 2).

- Position of Fig. 2

The following closed fullerene cage by size is C_{26}, of which there is only one classical closed-cage isomer. The highest possible symmetry of C_{26} is D_{3h}. The C_{26} fullerene cage comprises three consecutively connected hexagons and 12 pentagons. A ring is formed by connecting hexagons. Pentagons have a structure that could form bridges to these rings. Table S3 provides all calculation results such as optimization energy for each multiplicity, symmetry, and geometry for C_{26} fullerene cage. The researchers could not get a negative frequency in the frequency calculations of this fullerene cage. The results indicated that the most stable state of C_{26} fullerene cage determined the quintet spin multiplicity for neutral state, quartet spin multiplicity for anionic case, and sextet spin multiplicity for cationic case. Figure 3 showed the optimized geometry (a), Mulliken charge distribution (b), MEP counter (c), and HOMO-LUMO plot (d) of the most stable isomer of the C_{26} fullerene cage.

As seen in Fig. 3, the Mulliken atomic charges on C in the C_{26} fullerene cage were divided into four groups: -0.145 a.u. (six atoms in dark red color), 0.290 a.u. (twelve atoms in green color), -0.434 a.u. (six atoms in red color), and − 0.001 a.u. (two atoms in black color). Balevicius [25] et al. put forth that the HOMO and LUMO energies of C_{26} fullerene cage were determined at -8.6 1 eV and − 4.64 eV, respectively. Because the most stable state of C_{26} fullerene cage determined the quintet spin multiplicity for neutral state, HOMO and LUMO of C_{26} fullerene cage could be designated as α and β orbitals. The researchers calculated − 6.135 eV (HOMO energy of the α orbital) and − 2.927 eV (LUMO energy of the α orbital), -5.929 eV (HOMO energy of the β orbital) and − 4.314 eV (HOMO energy of the β orbital).

To gain insight into the electronic properties of the lowest energy isomer, we evaluated the IP, EA, and VDE of C_{26} fullerene cage at the DFT/CAM-B3LYP level (Table 1). In the present study, the researchers obtained at 7.443 eV (IP), 2.618 eV, and 2.452 eV (adiabatic and vertical EA), 2.815 eV (Vertical detachment energy). Janjanpour [23] et al. reported that the IP and EA in the C_{26} fullerene cage were predicted at 2.95 eV and 3.34 eV by B3LYP/6–31 + G (d), respectively. An [26] et al. argued that the EA_{vert} of the most stable geometry of C_{26} fullerene cage were 2.72 eV.

The most stable geometry of the C_{26} fullerene cage possesses D_{3h} symmetry group. Regarding this structure, it could be stated that C_{26} had a very symmetrical structure. So, μ and β_0 components of the C_{26} fullerene cage were all zero. The $\bar{\alpha}$ of C_{26} fullerene cage was calculated as 34.14×10^{-24} esu and the $\Delta\alpha$ of C_{26} fullerene cage was calculated to be 5.588×10^{-24} esu by DFT/CAM-B3LYP level (Table 2).

- Position of Fig. 3

C_{28} fullerene plays an important role in theoretical studies on fullerenes smaller than C_{30}. Because the first member of the fullerene cage family having a magic number is the C_{28} fullerene cage. The

researchers reported that the C_{28} had two isomers with T_d and D_2 symmetry [27]. The researchers optimized the two isomer with different spin states to achieve the most stable geometry. According to the results of the optimization calculations, the isomer of T_d symmetry of the C_{28} fullerene cage had the most stable isomer. The C_{28} fullerene cage comprises 4 hexagons and 12 pentagons. The C_{28} has been reported to have a tetrahedral structure, in which there are three isolated pentagons, one at each corner, which are not directly fused. In the isomer with T_d symmetry, we reported that the most stable state of C_{28} fullerene cage determined the quintet spin multiplicity for neutral state and quartet spin multiplicities for ionic cases. The researchers could not get negative frequency in the frequency calculations of this structure. Table S4 presents all calculation results such as optimization energy for each multiplicity, symmetry, and geometry for C_{28} fullerene cage. Figure 4 demonstrated the optimized geometry (a), Mulliken charge distribution (b), MEP counter (c), and HOMO-LUMO plot (d) of the most stable isomer of the C_{28} fullerene cage.

As seen in Fig. 4, the Mulliken atomic charges on C in the C_{28} fullerene cage were divided into three groups: 0.318 a.u. (twelve atoms in green color), -0.109 a.u. (twelve atoms in dark red color), and – 0.627 a.u. (four atoms in red color). The HOMO-LUMO gap of the neutral C_{28} fullerene cage with Td symmetry was predicted at 4.201 eV for alpha orbital and 2.321 eV for beta molecular orbital by DFT/B3LYP level. These values were quite large when compared to the values of those of C_{60} and C_{70} fullerene cages.

Castro [28] et al. have put forward that the IP and EA for C_{28} fullerene cage would contribute to the understanding of its behavior in electron detachment and electron affinity situations. The calculated IP and EA_{Ad} were obtained as 7.69 eV and 3.39 eV. The results of the present study showed that 8.349 eV and 2.864 eV values were determined as IP and EA_{Ad} by DFT/CAM-B3LYP level. EA_{vert} were obtained at 2.733 eV and 3.007 eV for VDE by DFT/CAM-B3LYP level (Table 1).

In the present study, we calculated the $\bar{\alpha}$ of C_{28} fullerene cage as 35.99 $x10^{-24}$ esu. We note it is consistent with the value 40.44$x10^{-24}$ esu calculated by Sabirov et al. [29]. Since C_{28} fullerene cage has a high symmetry (T_d symmetry), all components of the μ and β_0 values are found as zero (Table 2).

- Position of Fig. 4

3.2. C_{3N} (N:0, 2, 4, 6, and 8) fullerenes

Based on the DFT calculation results, three C_{30} isomers were theoretically differentiated by D_{5h}-I-C_{30} isomer, C_{2v}-II-C_{30} isomer, and C_{2v}-III-C_{30} isomer. Table S5 provides all calculation results such as optimization energy for each multiplicity, symmetry, and geometry for C_{30} fullerene cages. Accordingly, the ground state C_{2v}-II-C_{30} isomer with singlet multiplicity was more stable than C_{2v}-I-C_{30} and D_{5h}-I-C_{30} isomers. The relative energy of C_{2v}-I-C_{30} and D_{5h}-I-C_{30} isomers determined as 28 kcal mol^{-1} and 55.81

kcal mol^{-1}. The C_{30} cage comprises 5 hexagons and 12 pentagons. The researchers could not get negative frequency in the frequency calculations of this structure. The most stable state of the cationic and anionic C_{2v}-II-C_{30} isomer obtained doublet spin multiplicity. Figure 5 showed the optimized geometry (a), Mulliken charge distribution (b), MEP counter (c), and HOMO-LUMO plot (d) of the most stable isomer of the C_{30} fullerene cage.

As seen in Fig. 5, the Mulliken atomic charges on C in the C_{30} fullerene cage were divided into ten groups. The three groups have positive Mulliken charges of 0.289 a.u., 0.188 a.u., and 0.183 a.u., and their colors on six atoms appear as green color and its shades. The three positively charged groups have a charge of 0.029 a.u., 0.008 a.u., and 0.001 a.u., and their colors on eleven atoms appear in dark green color and its shades. The two groups have negative Mulliken charges of -0.251 a.u. and − 0.195 a.u., and their colors on four atoms appear as red color and its shades. The three negatively charged groups have a charge of -0.078 a.u. and − 0.068 a.u., and their colors on eight atoms appear in dark red color and its shades.

Paul [5] et al. argued that 7.352 eV and 2.761 eV values were obtained as IP and EA by ωB97XD functional with 6–311 + G (d, p) basis set, respectively. In the present study, these properties were calculated at 7.808 eV for IP and 3.559 eV for EA_{ad} by DFT/CAM-B3LYP level. Moreover, 3.385 eV and 3.689 eV were determined as EA_{vert} and VDE, respectively (Table 1). Paul et al. [5] reported that the μ of C30 fullerene cage was calculated at 0.12 Debye by B3LYP functional with 6–311 + G (d, p) basis set. In our calculations, this value was predicted at 0.119 Debye by DFT/CAM-B3LYP level. In the same study of Paul et al. [5], $\bar{\alpha}$ value of C30 fullerene cage was calculated as 43.79 $x10^{-24}$ esu, and this value was determined as 40.151 $x10^{-24}$ esu in our study. Similarly, while the $\Delta\alpha$ value of C_{30} fullerene cage was determined as 17.64 $x10^{-24}$ esu by Paul et al. [5], it was determined as 5.438 $x10^{-24}$ esu in our study. The β_0 value of C_{30} fullerene cage was obtained at $0.76x10^{-30}$ esu (CAM-B3LYP/6-311 + G(d,p)) by Paul et al. [5] In our calculation results, this value was predicted as $2.062x10^{-30}$ esu (DFT/CAM-B3LYP) (Table 2).

- Position of Fig. 5

The C_{32} fullerene cage had six isomers. These isomers were named as D_3-VI-C_{32}, C_2-IV-C_{32}, C_2-I-C_{32}, D_2-II-C_{32}, D_{3d}-III-$C_{32,}$ and D_{3h}-V-C_{32} fullerene cages. Table S6 presents all calculation results such as optimization energy for each multiplicity, symmetry, and geometry for C_{32} fullerene cages. According to DFT results, D_3-VI-C_{32} fullerene cage with singlet multiplicity was the most stable among the C_2-IV-C_{32}, C_2-I-C_{32}, D_2-II-C_{32}, D_{3d}-III-$C_{32,}$ and D_{3h}-V-C_{32} fullerene cages. Relative energies of the all C_{32} fullerene cages reported 25.74 kcal mol^{-1} (C_2-IV-C_{32}), 54.59 kcal mol^{-1} (C_2-I-C_{32}), 65.59 kcal mol^{-1} (D_2 -II-C_{32}), 74.24 kcal mol^{-1} (D_{3d}-III-C_{32}), and 78.24 kcal mol^{-1} (D_{3h}-V-C_{32}) by DFT calculations. The C_{32} fullerene cage comprises 6 hexagons and 12 pentagons. The researchers could not obtain negative frequency in the frequency calculations of the most stable structure. Figure 6 showed the optimized geometry (a),

Mulliken charge distribution (b), MEP counter (c), and HOMO-LUMO plot (d) of the most stable isomer of the C_{32} fullerene cage.

As seen in Fig. 6, the Mulliken atomic charges on C in the C_{32} fullerene cage were divided into two groups. The Mulliken charges of the first group were 0.280 a.u. and 0.210 a.u. The charges were on twenty atoms and their color was green and its shades. The Mulliken charges of the second group were − 0.049 a.u., -0.097 a.u., -0.176 a.u., and − 0.503 a.u. The charges were on twelve atoms and their color was red and its shades. Lin et al. [30] reported that HOMO-LUMO energy gap of the lowest-energy of C_{32} fullerene cage with D_3 symmetry was obtained at 2.602 eV by means of B3LYP/6-31G(d,p) level. In the present study, the HOMO, LUMO and HOMO-LUMO gap energies of the C_{32} fullerene cage were determined at -6.624 eV, -4.014 eV, and 2.610 eV for DFT/B3LYP level. The C_{70} and C_{60} fullerene cages were much larger and much more stable than the C_{32} fullerene cage. However, neutral C_{32} seems to have a much larger HOMO-LUMO gap value than those of C_{70} (1.3 eV) and C_{60} (1.6 eV) [30].

The EA of C_{32} was experimentally reported as ∼2.8 eV [31]. In our theoretical results (DFT/CAM-B3LYP level), EA_{ad} of C_{32} fullerene cage was obtained at 3.025 eV. Similarly, its EA_{vert} was calculated as 2.769 eV. IP and VDE values of C_{32} fullerene cage were found as 8.178 eV and 3.305 eV by DFT/CAM-B3LYP level (Table 1). The $\bar{\alpha}$ and the $\Delta\alpha$ value of C_{30} fullerene cage were found 43.434x10^{-24} esu and 8.035 x10^{-24} esu by DFT/CAM-B3LYP level (Table 2). All components of μ and β_0 values were calculated as zero.

- Position of Fig. 6

There were six isomers for C_{34} fullerene cage. These isomers optimized by using the DFT/B3LYP level. Table S7 presents all calculation results such as optimization energy for each multiplicity, symmetry, and geometry of the C_{34} fullerene cages. These six isomers were determined according to their symmetry as follows: three C_2, two C_S, and one C_{3V}. In the DFT calculations, the most stable C_{34} fullerene cage was the C_2-V-C_{34} geometry with triplet multiplicity. Relative energies of other isomers with respect to the most stable geometry were determined at 13.661 kcal mol^{-1} (C_2-IV-C_{34}), 28.413 kcal mol^{-1} (C_s-II-C_{34}), 29.318 kcal mol^{-1} (C_S-III-C_{34}), 30.887 kcal mol^{-1} (C_{3V}-VI-C_{34}), and 73.936 kcal mol^{-1} (C_2-I-C_{34}) by DFT/B3LYP level. Figure 7 showed the optimized geometry (a), Mulliken charge distribution (b), MEP counter (c), and HOMO-LUMO plot (d) of the most stable isomer of the C_{34} fullerene cage.

The negative atomic charges on C in the C_{34} fullerene cage were determined at -0.146 a.u., -0.068 a.u., -0.047 a.u., -0.117 a.u., -0.021 a.u., -0.066 a.u., -0.436 a.u., -0.034 a.u., and − 0.278 a.u. (each charge was on two atoms.). These charges were shown in red color and its shades as seen in Fig. 7. The positive atomic charges on C in the C_{34} fullerene cage was found 0.222 a.u., 0.073 a.u., 0.261 a.u., 0.005 a.u.,

0.163 a.u., 0.313 a.u., 0.064 a.u., and 0.112 a.u. (each charge is on two atoms.). These charges were shown in green color and its shades in the Fig. 7.

S. A. Halim et al. [32] predicted the electronic structure and stability of C_{34} and transition metal doped C_{34} derivative by using B3PW91/6-31G(d) level. In their study, the HOMO, LUMO, and HOMO-LUMO gap energies of the C_{34} fullerene cage were reported as -5.53 eV, 4.06 eV, and 1.47 eV, respectively. In our calculations, the C_{34} fullerene cage had alpha and beta molecular orbitals because the most stable structure of C_{34} had triplet multiplicity. The HOMO energies of α and β orbitals were obtained as -5.693 eV and − 6.524 eV by DFT/B3LYP level. The LUMO energies of α and β orbitals were calculated as? -3.865 eV and − 4.376 eV. The HOMO-LUMO gap for α and β orbitals of C_{34} were found as 1.828 eV and 2.148 eV. S. A. Halim et al. [32] reported the calculation results of the IP, EA, chemical hardness, electronegativity, chemical potential, electrophilicity of pure $C_{34,}$ and transition metal doped C_{34}. In that study, these data were calculated according to Koopman's theorem. It was addressed that the estimated IP value was 5.530 eV and the estimated EA value was 4.057 eV by the B3PW91/6-31G(d) level. In our computational work, the IP, EA_{ad}, $EA_{vert,}$ and VDE values of C_{34} fullerene cage were obtained as 7.450 eV, 2.955eV, 3.062 eV and 3.163 eV, respectively (Table 1).

In the study by S.A. Halim et al. [32] all components of the μ, $\bar{\alpha}$, $\Delta\alpha$ and β_0 values of C_{34} fullerene cage were calculated and reported. In the same study, the $\bar{\alpha}$, the $\Delta\alpha$, μ, and β_0 values were also obtained by B3PW91/6-31G (d) level. In that study, 40.07 x10^{-24} esu, 8.613 x10^{-24} esu, 0.155 Debye, and 0.955 x10^{-30} esu values were determined as the $\bar{\alpha}$, $\Delta\alpha$, μ, and β_0, respectively. In the present study, 46.062 x10^{-24} esu, 8.103 x10^{-24} esu, 0.113 Debye, and 2.656 x10^{-30} esu values were determined as the $\bar{\alpha}$, $\Delta\alpha$, μ and β_0 by DFT/CAM-B3LYP level, respectively (Table 2).

- Position of Fig. 7

C_{36} was one of the magic-number small fullerenes detected by mass spectroscopy in the very early days. C_{36} had 15 conventional fullerene isomers. Table S8 presents all calculation results such as optimization energy for each multiplicity, symmetry, and geometry of the C_{36} fullerene. D_{6h} and D_{2d} isomers contained a minimum number of adjacent pentagons. Therefore, they were candidates for the most stable structure. In the DFT calculations, it was revealed that the D_{6h}-XV-C_{36} fullerene cage with triplet multiplicity case was the most stable structure.

The symmetry and relative energies of other structures were determined as 1.800 kcal mol^{-1} for D_{2D}-XIV-C_{36}, 6.727 kcal mol^{-1} for C_2-XII-C_{36}, 7.173 kcal mol^{-1} for C_{2V}-IX-C_{36}, 13.17 kcal mol^{-1} for C_2-XI-C_{36}, 24.42 kcal mol^{-1} for C_S-VIII-C_{36}, 31.98 kcal mol^{-1} for D_{2D}-VI-C_{36}, 37.01 kcal mol^{-1} for C_1-VII-C_{36}, 40.61 kcal mol^{-1} for D_{3H}-XIII-C_{36}, 47.86 kcal mol^{-1} for C_2-X-C_{36}, 59.02 kcal mol^{-1} for C_1-III-C_{36}, 76.27 kcal mol^{-1} for C_S-IV-C_{36}, 84.41 kcal mol^{-1} for C_2-I-C_{36}, 90.66 kcal mol^{-1} for D_2-V-C_{36} and 117.5 kcal mol^{-1} for D_2-II-C_{36}.

Figure 8 showed the optimized geometry (a), Mulliken charge distribution (b), MEP counter (c), and HOMO-LUMO plot (d) of the most stable isomer of the C_{36} fullerene cage.

As seen in Fig. 8, the Mulliken atomic charges on C in the C_{36} fullerene cage were divided into three groups: -0.057 a.u. (twelve atoms, red color), 0.052 a.u. (twelve atoms, green color), and 0.005 a.u. (twelve atoms, dark color). C_{36} fullerene cage had HOMO-LUMO gaps of 1.718 eV (alpha molecular orbital) and 1.744 eV (beta molecular orbital) which were calculated theoretically by DFT/B3LYP level. The HOMO-LUMO gap value (~ 1.7 eV) of C_{36} fullerene cage was determined close to those of C_{60} (1.6 eV) which was very stable and larger than itself.

Using photoelectron spectroscopy, the EA of the C_{36}^{-} anion in the gas phase was measured as 3.0 eV [31]. In theoretical study, EA and IP values of C_{36} fullerene cage with D_{6h} symmetry were calculated as 6.70 eV and 2.50 eV by B3LYP/6-31G(d) level[31]. In the present study, these properties were predicted as 7.335 eV (IP), 2.889 eV (EA_{ad}), 2.815 eV (EA_{vert}), and 2.962 eV (VDE) by DFT/CAM-B3LYP level (Table 1).

In the present study, the calculated the $\bar{\alpha}$ of C_{36} fullerene cage was obtained at 47.561 x10^{-24} esu by DFT/CAM-B3LYP level. Sabirov[29] et al. marked that the $\bar{\alpha}$ of C_{36} fullerene cage was 52.41 x10^{-24} esu. The $\Delta\alpha$ of C_{36} fullerene cage was calculated as 0.909 x10^{-24} esu by DFT/CAM-B3LYP level. Since C_{36} fullerene cage had a D_{6h} symmetry, all components of μ and β_0 values were found zero (Table 2).

- Position of Fig. 8

There were 17 isomers of C_{38} fullerene cage. Table S9 presented all calculation results, such as optimization energy for each multiplicity, symmetry, and geometry of the C_{38} fullerene cage. The symmetries of these isomers were determined as five C_2 symmetry, seven C_1 symmetry, two C_{2V} symmetry, one C_{3V} symmetry, one D_3 symmetry, and one D_{3H} symmetry. In the DFT calculations, it was revealed that the C_2-XVII-C_{38} fullerene cage with singlet multiplicity case was the most stable structure. The relative energies of the other isomers were calculated as 18.78 kcal mol^{-1} for C_2-XIII-C_{38} isomer, 23.339 kcal mol^{-1} for C_2-X-C_{38} isomer, 54.390 kcal mol^{-1} for C_2-VI-C_{38} isomer, 102.601 kcal mol^{-1} for C_2-I-C_{38} isomer, 26.738 kcal mol^{-1} for C_1-XIV-C_{38} isomer, 38.048 kcal mol^{-1} for C_1-VIII-C_{38} isomer, 41.387 kcal mol^{-1} for C_1-V-C_{38} isomer, 45.983 kcal mol^{-1} for C_1-XI-C_{38} isomer, 62.956 kcal mol^{-1} for C_1-III-C_{38} isomer, 69.114 kcal mol^{-1} for C_1-VII-C_{38} isomer, 77.544 kcal mol^{-1} for C_1-IV-C_{38} isomer, 87.537 kcal mol^{-1} for C_{2V}-XII-C_{38} isomer, 50.486 kcal mol^{-1} for C_{2V}-XV-C_{38} isomer, 25.978 kcal mol^{-1} for C_{3V}-XVI-C_{38} isomer, 70.905 kcal mol^{-1} for D_3-IX-C_{38} isomer, and 131.451 kcal mol^{-1} for D_{3H}-II-C_{38} isomer. Figure 9 showed the optimized geometry (a), Mulliken charge distribution (b), MEP counter (c), and HOMO-LUMO plot (d) of the most stable isomer of the C38 fullerene cage.

The negative atomic charges on C in the C_{38} fullerene cage were determined at -0.003 a.u., -0.009 a.u., -0.012 a.u., -0.013 a.u., -0.020 a.u., -0.040 a.u., -0.045 a.u., -0.050 a.u., -0.080 a.u., -0.104 a.u., -0.114 a.u., -0.130 a.u., -0.140 a.u., and − 0.16 a.u. (each charge is on two atoms.). These charges were shown in red and its shades in Fig. 9. The positive atomic charges on C in the C_{38} fullerene cage were found as 0.189 a.u., 0.083 a.u., 0.189 a.u., 0.247 a.u., and 0.218 a.u. (each charge is on two atoms.). These charges were shown in green and its shades in the Fig. 9. We found HOMO, LUMO, and HOMO-LUMO gap values of C_2-XVII-C_{38} isomer in the C_{38} fullerene cages as -5.832 eV, -4.064 eV, and 1.768 eV by DFT/B3LYP level. The HOMO-LUMO gap of C_2-XVII-C_{38} isomer was close to those of C_{60} (1.6 eV).

In the present study, the IP, EA_{ad}, $EA_{vert,}$ and VDE properties of C_{38} fullerene cage were calculated at 7.335 eV, 2.889 eV, 2.815 eV, and 2.962 eV by DFT/CAM-B3LYP level respectively (Table 1). The obtained $\bar{\alpha}$ of C_{38} fullerene cage was at 49.958 x10^{-24} esu by DFT/CAM-B3LYP level. The $\Delta\alpha$ of C_{38} fullerene cage was predicted as 5.917 x10^{-24} esu by DFT/CAM-B3LYP level. μ was determined at 0.033 Debye, the β_0 values were found 0.289 x10^{-30} esu by DFT calculations (Table 2).

- Position of Fig. 9

3.3. Comparison of some properties

In conceptual DFT, Fukui functions could be employed as local descriptors to predict nucleophilic and electrophilic attacks. As seen in Figure S1, Fukui functions of C_N (N = 20, 24, 26, 28, 30, 32, 34, 36, and 38) fullerene cages are exhibited. Since the results from the Hirshfeld charge were reliable, the researchers calculated the Fukui function using the Hirshfeld charge. The nucleophilic region covered by the negative isosurfaces were the regions colored in blue and the electrophilic region covered by the positive isosurfaces were colored in green. As understood from the figure, both nucleophilic (blue areas in the Figures) and electrophilic (green areas in the Figures) regions were determined using the Hirshfeld charge of the carbon atoms in the fullerene. The images of the Fukui functions were obtained through the Multiwfn 3.8.8 program [33].

C_{60} was the most stable fullerene comprising 20 hexagons and 12 pentagons. Therefore, the focus of most of the experimental studies on fullerenes was C_{60} fullerene. In the present study, we compared the HOMO LUMO values of the calculated fullerenes with the data of C_{60}. The HOMO-LUMO gaps of fullerenes calculated at the DFT B3LYP/6-311G (d,p) level have been proved to be useful in determining their stabilities. Fullerenes with HOMO-LUMO gap value greater than 1.3 eV had high stability. However, HOMO-LUMO gap value less than this value showed low stability. The studied fullerenes had HOMO-LUMO gap values greater than 1.3 eV.

While the C_{26} and C_{28} fullerene cages were the most stable in quartet multiplicities, the C_{34} and C_{36} fullerene cages were the most stable in triplet multiplicities. As seen in Fig. 10, as the multiplicity

increased, especially the LUMO value of the α orbitals increased. Therefore, we compared the C_{60} values with fullerenes that were stable only at the singlet multiplicity. Since the C_{26}, C_{28}, C_{34} and C_{36} fullerene cages were found to be stable at high multiplicities, we did not make comparisons with the C_{60} data.

Wang et al. [34] calculated the HOMO, LUMO, and HOMO-LUMO gap values of C_{60} by B3LYP/6-311G(d,p) level. In their study, -6.402 eV, -3.658 eV, and 2.744 eV were predicted as HOMO, LUMO, and HOMO-LUMO gap of C_{60}, respectively. In the present study, the C_{32} fullerene cage had the highest HOMO-LUMO gap value (2.610 eV). C_{32} is a magic number carbon cluster that always gives very intense signals in gas phase experiments. In PES studies, it is stated that the neutral C_{32} molecule has a HOMO-LUMO gap comparable to C_{70} and C_{60} [31]. In the present study, the HOMO-LUMO value of the C_{32} fullerene cage closest to the HOMO-LUMO value of C_{60} was determined by DFT calculation.

- Position of Fig. 10
- Position of Table 3

Table 3
Comparison of HOMO-LUMO energies of studied neutral fullerenes with C60.

Fullerenes	E_{HOMO} (eV)		E_{LUMO} (eV)		$\Delta E_{HOMO-LUMO}$ (eV)	
C20	-5.442		-3.506		1.936	
C24	-6.050		-4.221		1.829	
C26	-6.135 *	-5.929 **	-2.927 *	-4.314 **	3.208 *	1.615 **
C28	-6.495 *	-6.606 **	-2.293 *	-4.285 **	4.202 *	2.321 **
C30	-6.391		-4.098		2.293	
C32	-6.624		-4.014		2.610	
C34	-5.693 *	-6.524 **	-3.865 *	-4.376 **	1.828 *	2.148 **
C36	-5.683 *	-6.075 **	-3.902 *	-4.331 **	1.781 *	1.744 **
C38	-5.832		-4.064		1.768	
C60	-6.402		-3.658		2.744	
* denotes the energy of the α molecular orbital						
** denotes the energy of the β molecular orbital						

Veries et al. reported that the IP of C_{60} was experimentally determined to 7.58 eV by using single-photon ionization [35]. As seen in Fig. 11, the sequence of magnitude of the IP values was determined as C_{28} >

$C_{32} > C_{30} > C_{24} > C_{26} > C_{36} > C_{38} > C_{20}$. When evaluated on IP data, we slightly overestimated the values of C_{24}, C_{28}, $C_{30,}$ and C_{32} fullerene cages from the experimental value of C_{60}. The IP value of the other fullerene cage were calculated slightly smaller than the C_{60} experimental data. The most accurate EA of C_{60} was determined as 2.6835 eV by the high-resolution photoelectron imaging [36]. When compared to the previous studies on fullerenes with the EA value of C_{60}, only the C_{20} and C_{26} fullerene cages values were calculated slightly small while the other fullerene cages were calculated slightly larger. Overall, it could be stated that the IP and EA values of the studied fullerenes were compatible with the C_{60} data.

- Position of Fig. 11

Nabil et al. reported that the $\bar{\alpha}$ of C_{60} fullerene cage was calculated at $77.59x10^{-24}$ esu by CAM-B3LYP/6–31 + G(d,p) level [37]. Among the fullerenes studied, the smallest $\bar{\alpha}$ value was determined as $27.59x10^{-24}$ esu in C_{20} fullerene cage by DFT/CAM-B3LYP level. This value increased continuously for all fullerenes up to C_{38} fullerene. The $\bar{\alpha}$ value of C_{38} fullerene cage was determined as $49.95x10^{-24}$ esu by DFT/CAM-B3LYP level. Hyperpolarizability values of the C_{20}, C_{24}, C_{26}, C_{28}, $C_{32,}$ and C_{36} fullerene cages with zero dipole moment were found zero. The other fullerenes had small dipole moments and small hyperpolarizability values.

Density of state (DOS) pictograms were obtained from Gaussian curves of unit height. DOS pictograms was obtained using the Mulliken population analysis results. DOS pictograms of fullerenes were obtained using the GaussSum 2.2 program [38]. The full width at half maximum (FWHM) at half height was used as 0.3 eV. The spectra of the state densities, which carry the orbital information of the molecules and emerge with the Gaussian type curves, were presented in Fig. 14.1. The state density plots presented the population analysis per orbital. Figure S2 showed the DOS pictograms in the energy range − 20 to 0 eV. As seen in Figure S2, the DOS pictograms of the stable fullerenes in the singlet or high multiplicities were visualized. Total DOS pictograms in the singlet case and DOS pictograms of the α occupied and β virtual orbitals in the high multiplex case were created.

4. Conclusions

This study reported quantum chemical study of C_N (N = 20, 24, 26, 28, 30, 32, 34, 36, and 38) fullerene cages. More specifically, detailed structural, electronic, non-linear optical properties, Mulliken charge, density of state, and Fukui function analysis of these fullerenes were provided. In conclusion, the symmetries and multiplicities of the global minimum structure of these fullerene cages were found D_2 with singlet (C_{20}), D_6 with singlet (C_{24}), D_{3h} with quintet (C_{26}), T_d with quintet (C_{28}), C_{2v} with singlet (C_{30}), D_3 with singlet (C_{32}), C_2 with triplet (C_{34}), D_{6h} with triplet (C_{36}), and C_2 with singlet multiplicity (C_{38}). Hyperpolarizability values of the C_{20}, C_{24}, C_{26}, C_{28}, C_{32} and C_{36} fullerene cages with zero dipole moment were found zero. The smallest mean polarizability value was determined in C_{20} fullerene cage. This value

increased continuously for all fullerenes up to C_{38} fullerene. Succinctly, it could be stated that the ionization potential and electron affinity values of the studied fullerenes were compatible with the C_{60} data. The HOMO-LUMO value of the C_{32} fullerene cage closest to the HOMO-LUMO value of C_{60} was determined by DFT calculation.

Declarations

Credit Authorship Contribution Statement

K. Soyarslan: Investigation, Writing – review & editing

B. Ortatepe: Resources Writing – review & editing

B. Yurduguzel: Resources Writing – review & editing

M. T. Güllüoğlu: Resources Writing – review & editing

Y. Erdogdu: Investigation, Writing – original draft, review & editing, Supervision.

Declaration of Competing Interest

The authors declare that they have no known competing financial interests or personal relationships that could have appeared to influence the work reported in this paper.

Acknowledgment

The Quantum Chemical calculations reported in this paper were fully performed at Harran University High Performance Computing Center (Harran HPC resources).

References

1. H. Kroto, Rev. Mod. Phys. 69 (1997) 703 – 722. https://doi.org/10.1103/RevModPhys.69.703.
2. P.W. Dunk, N.K. Kaiser, M. Mulet-Gas, A. Rodríguez-Fortea, J.M. Poblet, H. Shinohara, C.L. Hendrickson, A.G. Marshall, H.W. Kroto, J. Am. Chem. Soc. 134 (2012) 9380–9389. https://doi.org/10.1021/ja302398h.
3. Y.-M. Chen, J. Shi, L. Rui, Q.-X. Guo, Journal of Molecular Structure: THEOCHEM. 907 (2009) 104–108. https://doi.org/10.1016/j.theochem.2009.04.038.
4. Q. Sun, Q. Wang, J.Z. Yu, K. Ohno, Y. Kawazoe, J. Phys.: Condens. Matter. 13 (2001) 1931–1938. https://doi.org/10.1088/0953-8984/13/9/315.
5. D. Paul, J. Deb, U. Sarkar, ChemistrySelect. 5 (2020) 6987–6999. https://doi.org/10.1002/slct.202001988.

6. M.J. Frisch, G.W. Trucks, H.B. Schlegel, G.E. Scuseria, M.A. Robb, J.R. Cheeseman, G. Scalmani, V. Barone, G.A. Petersson, H. Nakatsuji, X. Li, M. Caricato, A.V. Marenich, J. Bloino, B.G. Janesko, R. Gomperts, B. Mennucci, H.P. Hratchian, J.V. Ortiz, A.F. Izmaylov, J.L. Sonnenberg, D. Williams-Young, F. Ding, F. Lipparini, F. Egidi, J. Goings, B. Peng, A. Petrone, T. Henderson, D. Ranasinghe, V.G. Zakrzewski, J. Gao, N. Rega, G. Zheng, W. Liang, M. Hada, M. Ehara, K. Toyota, R. Fukuda, J. Hasegawa, M. Ishida, T. Nakajima, Y. Honda, O. Kitao, H. Nakai, T. Vreven, K. Throssell, J.A. Montgomery, J.J.E. Peralta, F. Ogliaro, M.J. Bearpark, J. J. Heyd, E.N. Brothers, K.N. Kudin, V.N. Staroverov, T.A. Keith, R. Kobayashi, J. Normand, K. Raghavachari, A.P. Rendell, J.C. Burant, S.S. Iyengar, J. Tomasi, M. Cossi, J.M. Millam, M. Klene, C. Adamo, R. Cammi, J.W. Ochterski, R.L. Martin, K. Morokuma, O. Farkas, J.B. Foresman, D.J. Fox, Gaussian 16, Revision B.01, Gaussian, Inc., Wallingford CT, 2016.
7. A.D. Becke, J. Chem. Phys. 98 (1993) 5648–5653.
8. C. Lee, W. Yang, R. G. Parr, Phys. Rev. B. 37 (1988) 785–789.
9. T. Yanai, D.P. Tew, N.C. Handy, Chemical Physics Letters. 393 (2004) 51–57. https://doi.org/10.1016/j.cplett.2004.06.011.
10. R. Krishnan, J.S. Binkley, R. Seeger, J.A. Pople, The Journal of Chemical Physics. 72 (1980) 650–654. https://doi.org/10.1063/1.438955.
11. Mitsuho Yoshida, Fullerene Structure Library, (n.d.). https://nanotube.msu.edu/fullerene/fullerene-isomers.html.
12. Y. Erdogdu, S. Erkoc, Jnl of Comp & Theo Nano. 9 (2012) 837–850. https://doi.org/10.1166/jctn.2012.2105.
13. S. Subashchandrabose, H. Saleem, Y. Erdogdu, Ö. Dereli, V. Thanikachalam, J. Jayabharathi, Spectrochimica Acta Part A: Molecular and Biomolecular Spectroscopy. 86 (2012) 231–241. https://doi.org/10.1016/j.saa.2011.10.029.
14. A. Atilgan, Ş. Yurdakul, Y. Erdogdu, M.T. Güllüoğlu, Journal of Molecular Structure. 1161 (2018) 55–65. https://doi.org/10.1016/j.molstruc.2018.01.080.
15. A.S. Rad, K. Ayub, Materials Research Bulletin. 97 (2018) 399–404. https://doi.org/10.1016/j.materresbull.2017.09.036.
16. Z. Wang, K. Lian, S. Pan, X. Fan, J. Comput. Chem. 26 (2005) 1279–1283. https://doi.org/10.1002/jcc.20268.
17. H. Prinzbach, A. Weiler, P. Landenberger, F. Wahl, J. Wörth, L.T. Scott, M. Gelmont, D. Olevano, B. v. Issendorff, Nature. 407 (2000) 60–63. https://doi.org/10.1038/35024037.
18. A.S. Rad, K. Ayub, Appl. Phys. A. 125 (2019) 430. https://doi.org/10.1007/s00339-019-2721-7.
19. S. Yang, C. L. Pettiette, J.Conceicao, O.Cheshnovsky, R. E.Smalley, 139 (1987) 233–238. https://doi.org/10.1016/0009-2614(87)80548-1.
20. L.S.Wang, J. Conceicao, C.M. Jin, R. E.Smalley, Chemical Physics Letters, 182 (1991) 5. https://doi.org/10.1016/0009-2614(91)80094-E.

21. X.-B. Wang, C.-F. Ding, L.-S. Wang, The Journal of Chemical Physics. 110 (1999) 8217–8220. https://doi.org/10.1063/1.478732.
22. F. Jensen, H. Koch, The Journal of Chemical Physics. 108 (1998) 3213–3217. https://doi.org/10.1063/1.475716.
23. M. Heidari Nezhad Janjanpour, M. Vakili, S. Daneshmehr, K. Jalalierad, F. Alipour, Chem. Rev. Lett. 1 (2018). https://doi.org/10.22034/crl.2018.85215.
24. N. Kosar, H. Tahir, K. Ayub, T. Mahmood, Journal of Molecular Graphics and Modelling. 105 (2021) 107867. https://doi.org/10.1016/j.jmgm.2021.107867.
25. L.M. Balevišius, E. Stumbrys, A. Tamulis, Fullerene Science and Technology. 5 (1997) 85–96. https://doi.org/10.1080/15363839708011974.
26. J. An, L.-H. Gan, J.-Q. Zhao, R. Li, J. Chem. Phys. (n.d.) 7.
27. J.-J. Adjizian, A. Vlandas, J. Rio, J.-C. Charlier, C.P. Ewels, Phil. Trans. R. Soc. A. 374 (2016) 20150323. https://doi.org/10.1098/rsta.2015.0323.
28. A. Muñoz-Castro, R. Bruce King, J. Comput. Chem. 38 (2017) 44–50. https://doi.org/10.1002/jcc.24518.
29. D. Sh. Sabirov, R.G. Bulgakov, Jetp Lett. 92 (2010) 662–665. https://doi.org/10.1134/S0021364010220054.
30. J. Lin, J. Hu, J.-R. Zhang, S.-Y. Wang, Y. Ma, X.-N. Song, Spectrochimica Acta Part A: Molecular and Biomolecular Spectroscopy. 212 (2019) 180–187. https://doi.org/10.1016/j.saa.2018.12.043.
31. X. Lu, Z. Chen, Chem. Rev. 105 (2005) 3643–3696. https://doi.org/10.1021/cr030093d.
32. S.A. Halim, Int. J. Nano Dimens., 9(4) (2018) 421-434.
33. T. Lu, F. Chen, J. Comput. Chem. 33 (2012) 580–592. https://doi.org/10.1002/jcc.22885.
34. H. Wang, Y. He, Y. Li, H. Su, J. Phys. Chem. A. 116 (2012) 255–262. https://doi.org/10.1021/jp208520v.
35. J. de Vries, H. Steger, B. Kamke, C. Menzel, B. Weisser, W. Kamke, I.V. Hertel, , Chemical Physics Letters. 188 (n.d.) 4.
36. D.-L. Huang, P.D. Dau, H.-T. Liu, L.-S. Wang, The Journal of Chemical Physics. 140 (2014) 224315. https://doi.org/10.1063/1.4881421.
37. N. Omri, Y. Bu, J. Phys. Chem. A. 125 (2021) 106–114. https://doi.org/10.1021/acs.jpca.0c08533.
38. N.M. O'boyle, A.L. Tenderholt, K.M. Langner, J. Comput. Chem. 29 (2008) 839–845. https://doi.org/10.1002/jcc.20823.

Figures

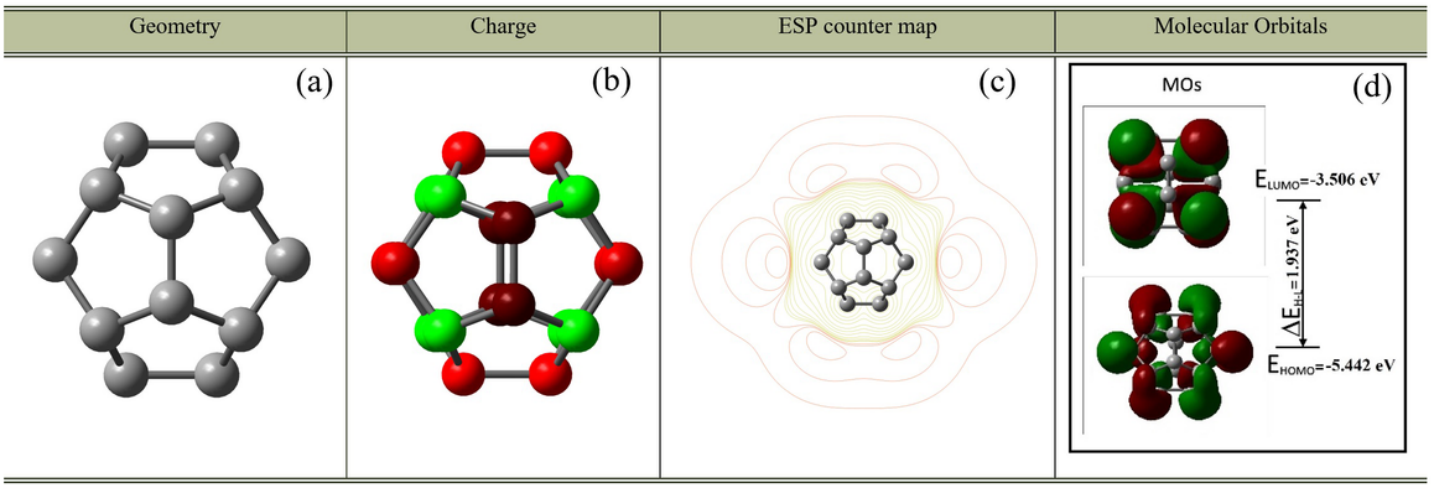

Figure 1

Geometry, Mulliken charge, ESP counter map and HOMO, LUMO plots of C20 fullerene cage

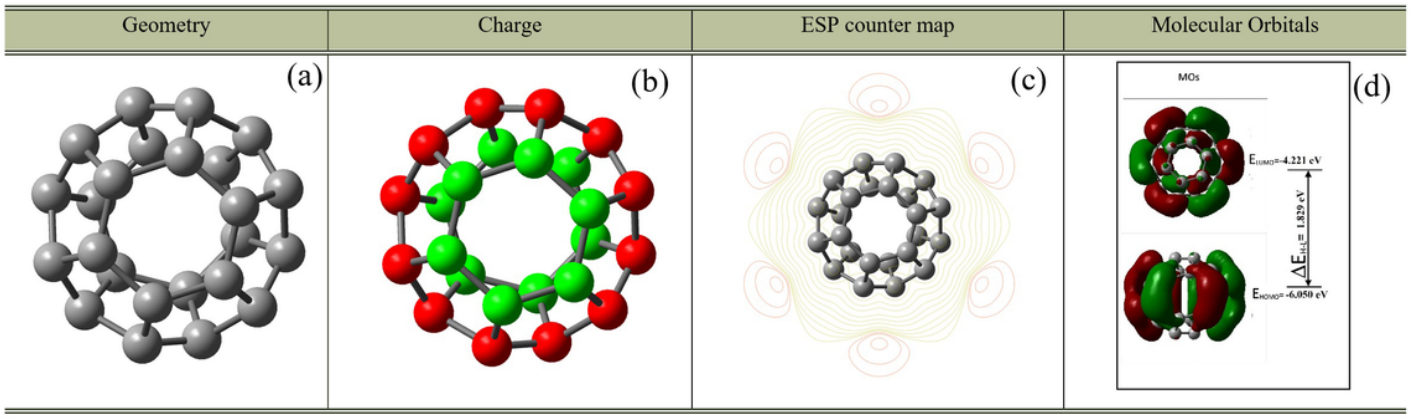

Figure 2

Geometry, Mulliken charge, ESP counter map and HOMO, LUMO plots of C24 fullerene cage

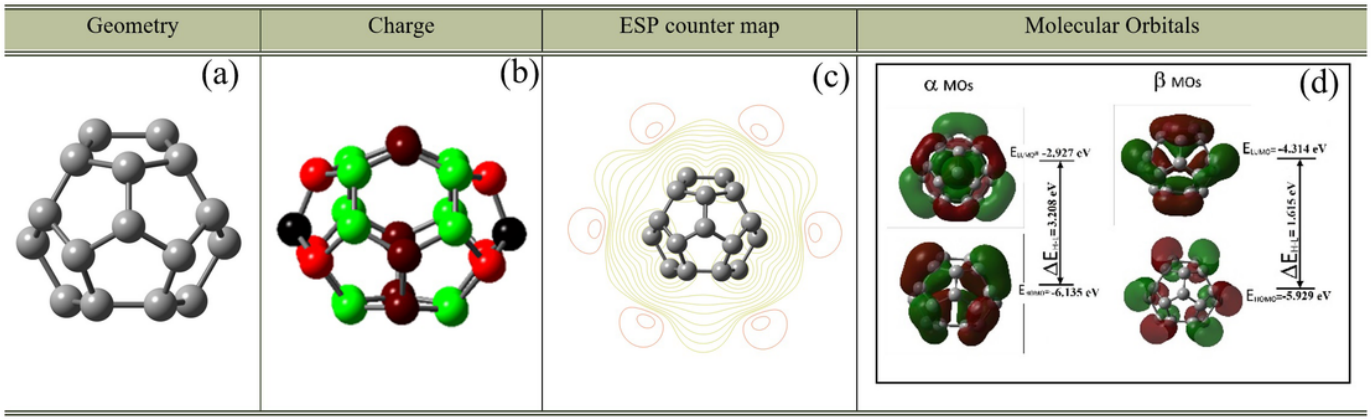

Figure 3

Geometry, Mulliken charge, ESP counter map and HOMO, LUMO plots of C26 fullerene cage

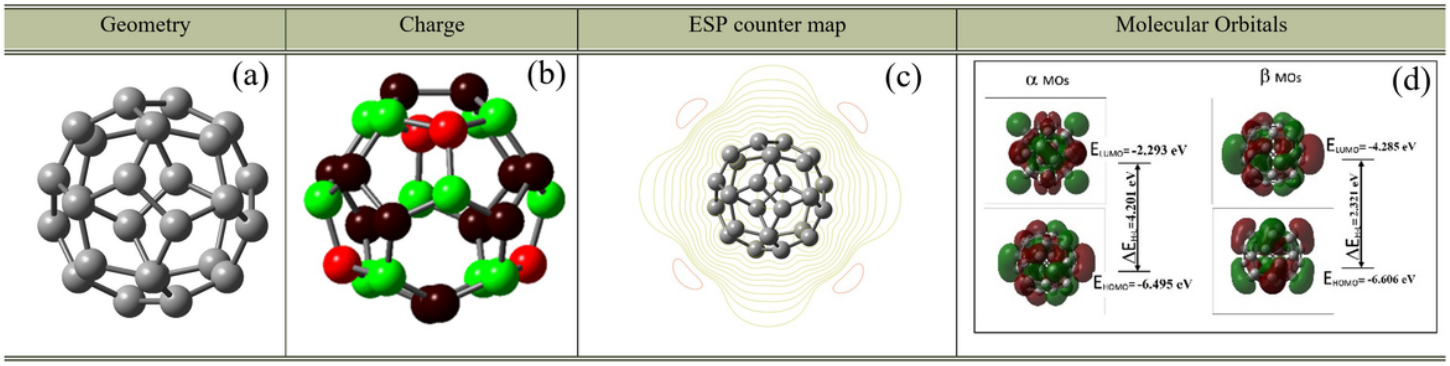

Figure 4

Geometry, Mulliken charge, ESP cour map and HOMO, LUMO plots of C28 fullerene cage

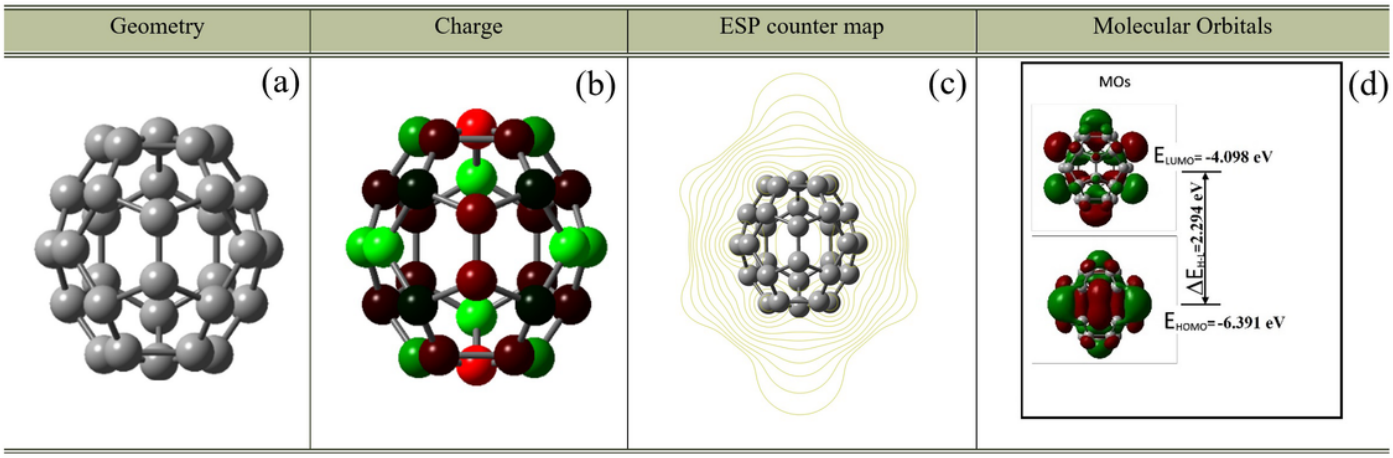

Figure 5

Geometry, Mulliken charge, ESP counter map and HOMO, LUMO plots of C30 fullerene cage

Figure 6

Geometry, Mulliken charge, ESP counter map and HOMO, LUMO plots of C32 fullerene cage

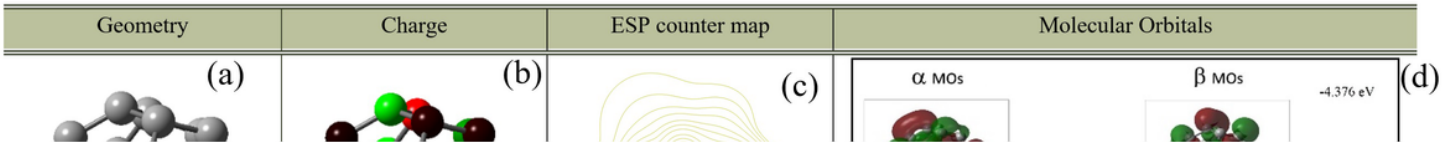

Figure 7

Geometry, Mulliken charge, ESP counter map and HOMO, LUMO plots of C34 fullerene cage

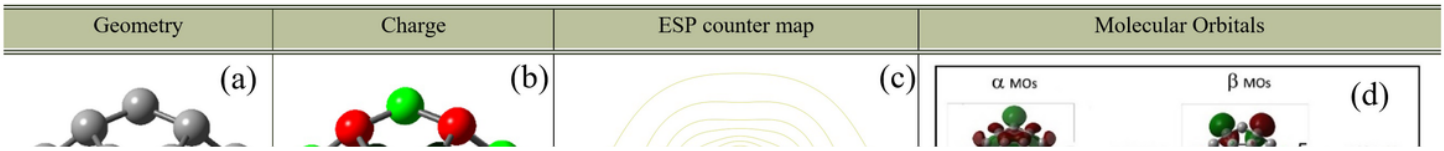

Figure 8

Geometry, Mulliken charge, ESP counter map and HOMO, LUMO plots of C36 fullerene cage

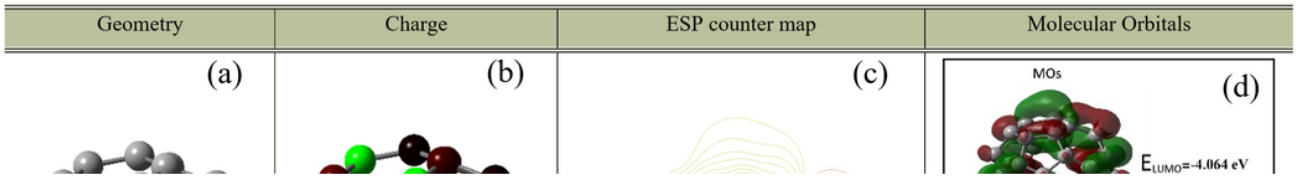

Figure 9

Geometry, Mulliken charge, ESP counter map and HOMO, LUMO plots of C38 fullerene cage

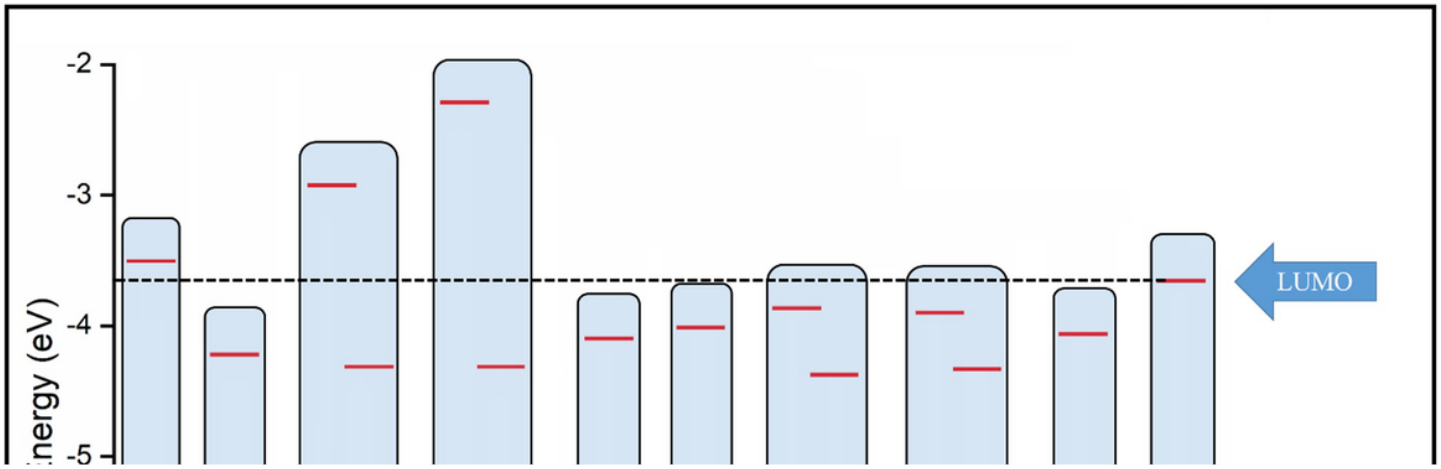

Figure 10

HOMO, LUMO, and HOMO-LUMO gaps of the fullerene cages

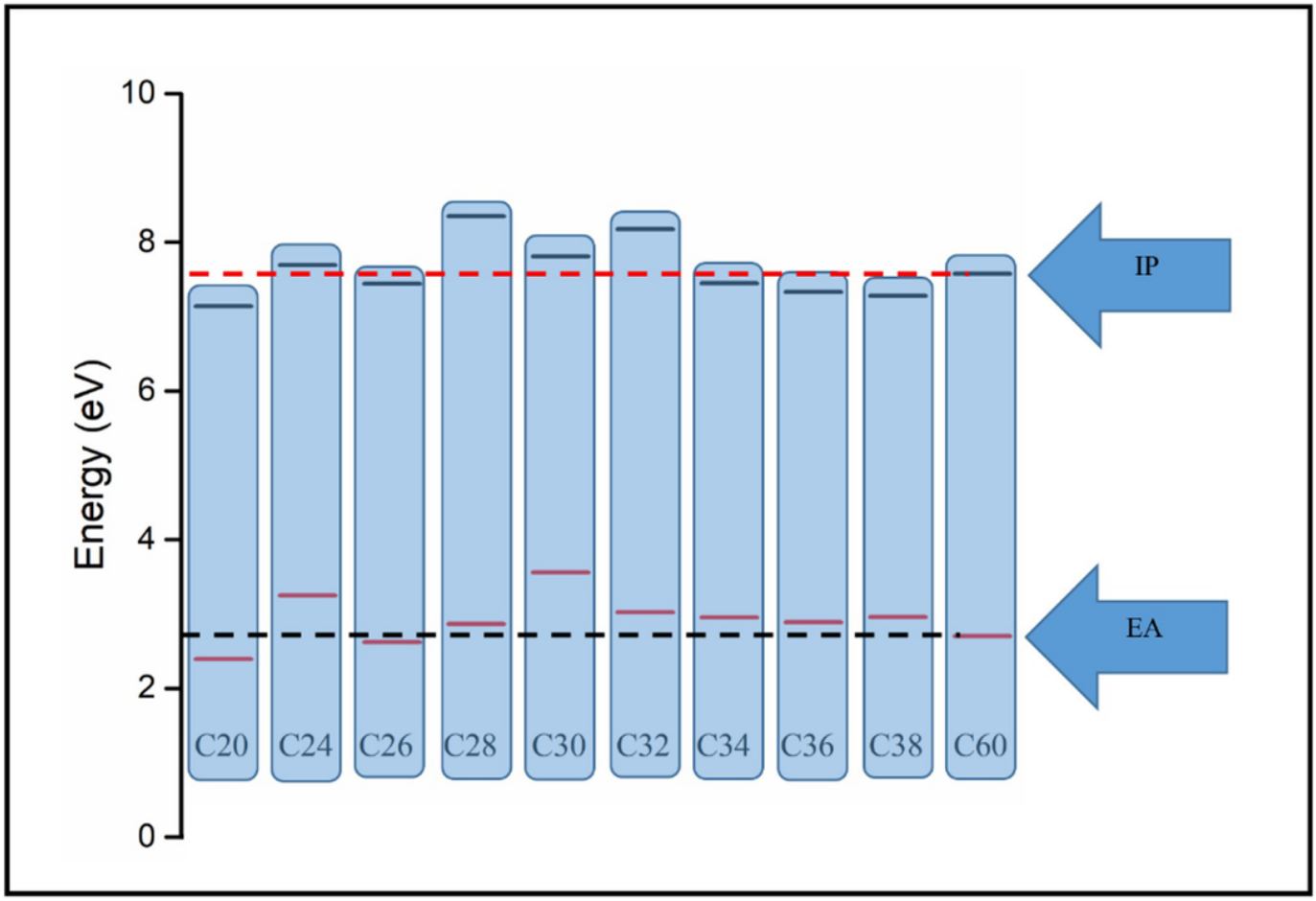

Figure 11

Comparison of IP and EA of fullerenes with C60

Supplementary Files

This is a list of supplementary files associated with this preprint. Click to download.

- Supp.Mat..docx